Tunable high-order harmonic generation and the role of the folded quantum path

Zhinan Zeng, Ya Cheng,* Yuxi Fu, Xiaohong Song, Ruxin Li,† and Zhizhan Xu‡
State Key Laboratory of High Field Laser Physics, Shanghai Institute of Optics and Fine Mechanics, CAS, P.O. Box 800-211, Shanghai 201800, China

(Received 24 September 2007; published 21 February 2008)

We theoretically demonstrate the selective enhancement of high-order harmonic generation (HHG) in two-color laser fields consisting of a single-cycle fundamental wave (800 nm wavelength) and a multicycle subharmonic wave (2400 nm wavelength). By performing time-frequency analyses based on a single-active-electron model, we reveal that such an enhancement is a result of the modified electron trajectories in the two-color field. Furthermore, we show that selectively enhanced HHG gives rise to a bandwidth-controllable extreme ultraviolet supercontinuum in the plateau region, facilitating the generation of intense single isolated attosecond pulses.

DOI: 10.1103/PhysRevA.77.023416 PACS number(s): 33.80.Rv, 42.65.Ky, 42.65.Re

I. INTRODUCTION

High-order harmonic generation (HHG) has shown great potential to become a coherent radiation source in the soft x-ray regime due to its intrinsically high spatial and temporal coherence [1]. For implementing this light source in a broad range of fields such as nanolithography, high-resolution imaging, extreme ultraviolet (xuv) interferometry, and so on, control of both the wavelength and the bandwidth is necessary. Precise control of the HHG wavelength and bandwidth is usually not a trivial task. Currently, the most frequently used techniques involve using filters or gratings for separating the wavelengths [2,3]; however, such methods usually cause significant optical loss in the soft x-ray regime. A more sophisticated method is to use the phase-matching technique in the HHG process, which employs the propagation effect for coherently building up an intense xuv radiation near a specific frequency [4]. Unfortunately, at present, the phase-matching technique is still only effective for relatively long wavelengths with photon energies less than 100 eV [5]. In this paper, we propose a purely optical approach to selectively enhance the HHG. The wavelength-selective enhancement can virtually be obtained in both the plateau and cutoff regions of the HHG spectrum with the highest enhancement factors up to one order of magnitude (in comparison with the remaining unenhanced region). Moreover, we reveal that this enhancement effect is a result of modified electron trajectories in the complex optical wave form offered by the two-color laser field.

II. GENERATION OF TUNABLE HIGH-ORDER HARMONICS

In our simulation, a 3-fs, 800-nm pulse and a 64-fs, 2400-nm pulse are synthesized to serve as the driving pulse. Technically, a 2400-nm laser pulse can be generated with an optical parametric amplifier (OPA), and its duration has little effect on the simulation result as long as a multiple-optical-cycle pulse is chosen. On the other hand, the single-cycle-scale, 800-nm laser pulse used in our simulation is currently still not available, while we are optimistic about that such light sources will become a reality in the near future due to the rapid development of the ultrafast laser technology [6,7]. The model atom used is argon (Ar). The method of the simulation has detailed description in Refs. [1,8], which is based on a single-active-electron approximation and has been widely employed for HHG simulation. The high-harmonic spectrum can be obtained by Fourier-transforming the time-dependent dipole acceleration. The expression of the synthesized field can be written as

$$E_L = E_1 \exp[(-2\ln 2)t^2/\tau_1^2]\cos(\omega_1 t) + E_2 \exp[(-2\ln 2)(t-t_0)^2/\tau_2^2]\cos[\omega_2(t-t_0)], \quad (1)$$

where E_1 and E_2 are the amplitudes of the electric fields of the 800-nm and 2400-nm laser pulses, respectively, and ω_i and τ_i $(i=1,2)$ are the corresponding frequencies and pulse durations. The time t_0 determines the time delay between the two pulses. First, the intensities of the 3-fs, 800-nm laser pulse and the 2400-nm pulse are chosen as 3×10^{14} W/cm^2 and 1×10^{14} W/cm^2, respectively. We present the HHG spectra calculated with several different time delays of t_0=0.75, 1, 1.25, 1.5, 1.75, and 2 fs as shown in Fig. 1. Interestingly, although these HHG spectra show nearly the same cutoff energies at ~200 eV, a phenomenal enhancement of a narrow-band xuv radiation with a bandwidth ranging from 3 to 10 eV can be observed at different position of each HHG spectrum. To the best of our knowledge, such an interesting phenomenon has never been reported in any HHG literature yet. For each time delay used in our simulation, the enhancement factor is almost one order of magnitude. Further, the central frequency of the enhanced xuv radiation can be continuously shifted from the beginning of HHG plateau to the cutoff region by scanning the time delay, leading to a wide tuning range spanning from ~50 to ~150 eV. However, if the time delay increases further beyond one-quarter of the period of the 2400-nm pulse, this selective enhancement effect will disappear.

*ycheng-45277@hotmail.com
†ruxinli@mail.shcnc.ac.cn
‡zzxu@mail.shcnc.ac.cn

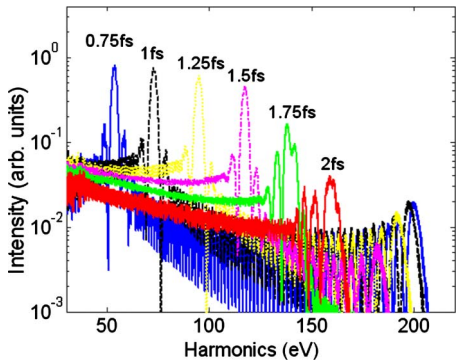

FIG. 1. (Color online) High-order harmonic spectra generated by synthesized field consisting of a 3-fs, 800-nm pulse and a 2400-nm pulse at different time delays.

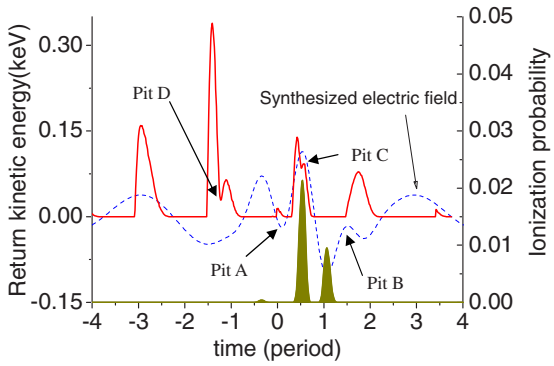

FIG. 3. (Color online) The electric field of the synthesized two-color laser field (dashed curve, time delay=1.5 fs), and the electron return energy time (solid curve) as well as the ionization probability as a function of the time (gray solid curve).

III. ROLE OF THE FOLDED QUANTUM PATH

In order to get the insight into this interesting phenomenon, we perform time-frequency analyses of the above HHG processes for different time delays, as shown in Fig. 2. It is well known that a HHG process mainly includes three steps [9]: namely, (i) tunnel ionization of the electron at the peak of electric field, (ii) excursion of the free electron in the oscillating laser field until being driven back to its parent ion, and (iii) recombination of the electron with the parent ion through the release of an xuv photon. In this classical picture of HHG, except for the cutoff photons (photons with energies close to the cutoff energy) which are contributed by the most energetic return electrons captured by the ion, the other xuv photons are all correlated in pairs due to the fact that the ionized electrons can gain equal kinetic energy upon return by traveling along either a "long" or a "short" trajectory in the laser field [10]. In accordance, time-frequency analysis has frequently shown that there are two quantum paths contributing to HHG in the plateau region [11]. On the contrary, the time-frequency diagrams shown in Fig. 2 clearly indicate that one can modify the electron trajectories in two-color laser fields so as to create additional quantum paths near the

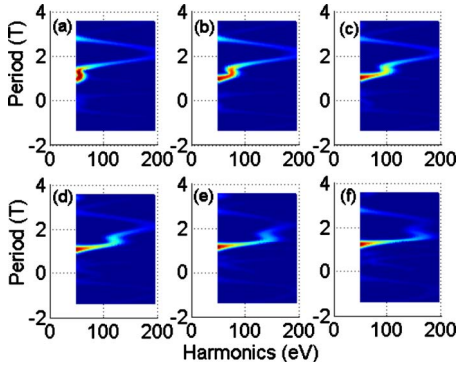

FIG. 2. (Color online) Time-frequency analysis diagrams for high-order harmonic spectra presented in Fig. 1. From (a) to (f), the time delay varies from 0.75 to 2 fs at a step of 0.25 fs.

folded regions of the time-frequency curves. It is the constructive interference between the multiple quantum paths that leads to the selectively enhanced xuv radiation. Nevertheless, when the time delay is increased to 1.75 and 2 fs, we observe in Fig. 1 that both the two selectively enhanced HHG spectra exhibit multipeak structures. In these two cases, due to the broadened time ranges of the folded areas and, more importantly, the higher xuv photon energies corresponding to the folded areas [see Figs. 2(e) and 2(f)], not only constructive, but also destructive interference can occur between the multiple quantum paths, resulting in a modulation of the selectively enhanced xuv spectra. Furthermore, it is clearly shown in Fig. 2 that, with an increase of the time delay, the folded area continuously shifts toward the high-frequency end of the time-frequency curve. This result is consistent with that shown in Fig. 1: namely, the longer the time delay, the higher the central frequency of the selectively enhanced xuv spectrum.

Further investigation shows that the folded electron trajectories are caused by the 3-fs, 800-nm laser pulse superimposed onto the 2400-nm pulse which substantially modifies the wave form of the light field. Shown in Fig. 3 are the electric field of the two-color laser pulse with a 1.5-fs time delay (dashed curve), the electron return energy as a function of its ionization time calculated by the classical three-step model [9] (solid curve) and the ionization probability (gray solid curve) calculated by the Ammosov-Delone-Krainov (ADK) model [12], all based on the laser parameters in Fig. 2(d). Obviously, the wave form of the two-color laser field fundamentally deviates from that of a single-color laser field, particularly evidenced by the two pits *A* and *B* presented in the two-color laser field, as shown in Fig. 3. The electric field approaches zero near these two pits. Because of these two pits, the electron return energy curve as a function of time (solid curve) in Fig. 3 also shows two pitlike structures, as indicated as pits *C* and *D*. Since the tunnel ionization is a highly nonlinear optical process which is very sensitive to the strength of the electric field, the strongest ionization of the Ar atom occurs at a time corresponding to the maximum peak electric field, as shown by the gray solid curve in Fig. 3.

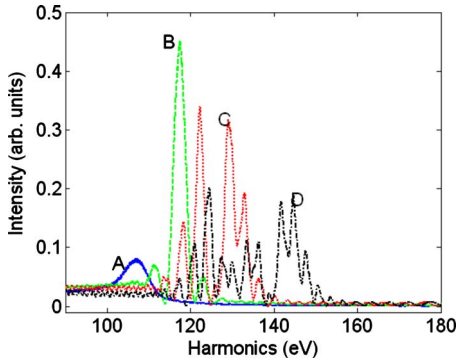

FIG. 4. (Color online) High-order harmonic spectra at different intensities of the 800-nm pulse for a fixed time delay of 1.5 fs. For curves $A-D$, the intensity of the 2400-nm pulse is fixed at 1×10^{14} W/cm^2, whereas the intensity of the 800-nm pulse varies from 2×10^{14} W/cm^2 to 5×10^{14} W/cm^2 at a step of 1×10^{14} W/cm^2.

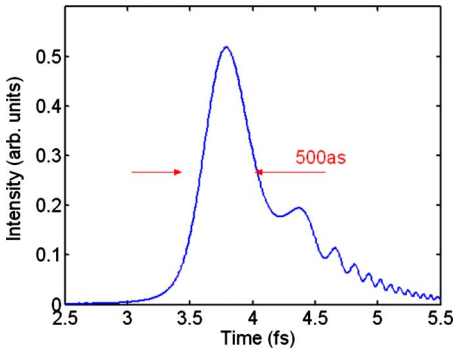

FIG. 5. (Color online) Temporal profile of the single attosecond pulse generated by Fourier synthesis of the high-order harmonics shown by the curve B in Fig. 4. Note that in this case, the low-energy photons (below ~100 eV) have been filtered out using a 50-nm-thick thin silver foil.

Thus, most of the ionized electrons which can contribute to the generation of selectively enhanced xuv radiation will travel along the classical electron trajectory with pit *C*. The similarity between the classical electron trajectory (solid curve) in Fig. 3 and the quantum trajectory in Fig. 2(d) provides a clear physical picture for the origin of folded quantum paths in two-color fields.

IV. CONTROL OF THE BANDWIDTH

Furthermore, we show that not only the central wavelength but also the bandwidth of the selectively enhanced xuv radiation can be controlled by adjusting the laser parameters in the above-mentioned two-color HHG scheme. From curves (A)–(D) in Fig. 4, we can see a continued increase in the bandwidth of the selectively enhanced xuv spectrum with increasing peak intensity of the 800-nm laser pulse. In addition, it is also found that for those relatively broad xuv spectra (curves *C* and *D* in Fig. 4) produced with the higher-intensity 800-nm laser pulses, the selectively enhanced xuv spectra are strongly modulated owing to the interference among the multiple quantum paths, as we have discussed above. Nevertheless, at the relatively low intensities of the 800-nm laser pulse, the selectively enhanced xuv radiation forms a spectrally smooth, bandwidth-limited xuv supercontinuum, which can be employed for directly synthesizing an intense attosecond pulse. It is important to note that the bandwidth of the selectively enhanced xuv spectrum shown by curve D in Fig. 1 is sufficiently broad for supporting a single xuv pulse of a few hundred attoseconds pulse duration. Therefore, we can use a thin silver foil (thickness =50 nm) to filter out all the low-energy xuv photons (below ~100 eV), which gives rise to a single ~500 as pulse obtained by performing an inverse Fourier transformation for the remaining xuv spectrum (>100 eV), as shown in Fig. 5. For the 50-nm-thick thin silver foil used here, the transmission will be higher than 80% at xuv photon energies above 100 eV. Thus, this approach would significantly improve the conversion efficiency for single-attosecond-pulse generation.

V. DISCUSSION AND CONCLUSIONS

In recent years, HHG in two-color laser fields has attracted significant attention, including an extension of the cutoff region [13], enhancement of the conversion efficiency [14], generation of single isolated attosecond pulses [15,16], measurement and control of the birth of attosecond pulses [17,18], and so on. In addition, it has been pointed out by an analytical model that high-order harmonics can be selectively enhanced in a circularly polarized two-color field [19] due to the existence of a selection rule [20]. Unlike these studies, we use the two-color few-cycle optical pulses mainly for the purpose of controlling the electron wave packet, which in turn substantially modifies the quantum electron trajectory. In this case, the selective enhancement originates from the constructive interference between the folded quantum trajectories owing to the superimposition of the 3-fs, 800-nm pulse. Therefore, two prerequisites of the selective enhancement must be fulfilled. First, the selectively enhanced harmonics must locate in a spectral range corresponding to the folding area in the quantum trajectory (see Fig. 2); second, the harmonics with a same frequency but emitted at different times must interfere with each other constructively. Generally speaking, within a certain range of time delay, the folding area in the quantum trajectory keeps on shifting towards the high-frequency end with an increase of the time delay between the two pulses. As a result, the longer the time delay, the higher the frequencies of the selectively enhanced harmonics.

In conclusion, we propose a purely optical method for generating a frequency-tunable and bandwidth-controllable coherent xuv radiation and reveal the physics underlying this unusual phenomenon by performing time-frequency analyses and classical modeling. By changing the time delay between the 800-nm single-cycle and the 2400-nm multicycle pulses, the broad tuning range of the selectively enhanced xuv radiation can cover the entire plateau region (e.g., from ~50 to ~150 eV). An intense single attosecond pulse can therefore be directly formed simply by filtering out the low-energy photons using a 50-nm-thick thin silver foil, which has a high transmission at photon energies above ~100 eV.

Furthermore, we show that the bandwidth of the selectively enhanced HHG can be easily adjusted by changing the intensity of the 800-nm laser pulse. Our time-frequency analyses based on the single-active-electron model reveal that such an enhancement is a result of the substantial modification of the electron trajectories in the laser field.

ACKNOWLEDGMENTS

This work is financially supported by National Basic Research Program of China (Grant No. 2006CB806000) and National Science Foundation of China (Grant No. 60578049 and 10523003).

[1] T. Brabec and F. Krausz, Rev. Mod. Phys. **72**, 545 (2000).
[2] L. B. Da Silva *et al.*, Phys. Rev. Lett. **74**, 3991 (1995).
[3] J. B. M. Warntjes *et al.*, Opt. Lett. **16**, 1463 (2001).
[4] V. Tosa, E. Takahashi, Y. Nabekawa, and K. Midorikawa, Phys. Rev. A **67**, 063817 (2003).
[5] X. Zhang *et al.*, Nat. Phys. **3**, 270 (2007).
[6] A. L. Cavalieri *et al.*, New J. Phys. **9**, 242 (2007).
[7] V. Pervak *et al.*, Appl. Phys. B: Lasers Opt. **87**, 5 (2007).
[8] X. Song, Z. Zeng, Y. Fu, B. Cai, R. Li, Y. Cheng, and Z. Xu, Phys. Rev. A **76**, 043830 (2007).
[9] P. B. Corkum, Phys. Rev. Lett. **71**, 1994 (1993).
[10] M. Bellini, C. Lynga, A. Tozzi, M. B. Gaarde, T. W. Hansch, A. L'Huillier, and C.-G. Wahlstrom, Phys. Rev. Lett. **81**, 297 (1998).
[11] X. M. Tong and Shih-I Chu, Phys. Rev. A **61**, 021802(R) (2000).
[12] M. V. Ammosov, N. B. Delone, and V. P. Krainov, Sov. Phys. JETP **64**, 1191 (1986).
[13] T. Pfeifer, L. Gallmann, M. J. Abel, P. M. Nagel, D. M. Neumark, and S. R. Leone, Phys. Rev. Lett. **97**, 163901 (2006).
[14] T. T. Liu, T. Kanai, T. Sekikawa, and S. Watanabe, Phys. Rev. A **73**, 063823 (2006).
[15] Y. Oishi, M. Kaku, A. Suda, F. Kannari, and K. Midorikawa, Opt. Express **14**, 7230 (2006).
[16] Z. Zeng, Y. Cheng, X. Song, R. Li, and Z. Xu, Phys. Rev. Lett. **98**, 203901 (2007).
[17] N. Dudovich *et al.*, Nat. Phys. **2**, 781 (2006).
[18] W. Cao, P. Lu, P. Lan, X. Wang, and Y. Li, Phys. Rev. A **75**, 063423 (2007).
[19] F. Ceccherini, D. Bauer, and F. Cornolti, Phys. Rev. A **68**, 053402 (2003).
[20] O. E. Alon, V. Averbukh, and N. Moiseyev, Phys. Rev. Lett. **80**, 3743 (1998).